Preprint
UCRL-JC-147825

# Multiple Film Plane Diagnostic for Shocked Lattice Measurements

*D.H. Kalanta, E. Bringa, M. Caturla, J. Colvin, K.T. Lorenz, M. Kumar, J. Stolken, A.M. Allen, K. Rosolankova, J.S. Wark, M.A. Meyers, M. Schneider, and T.R. Boehly*

This article was submitted to the 14th American Physical Society Topical Conference on High Temperature Plasma Diagnostics, Madison, Wisconsin, July 8-11, 2002

*U.S. Department of Energy*

Lawrence Livermore National Laboratory

**July 2, 2002**

**Multiple Film Plane diagnostic for shocked lattice measurements**[1]

Daniel H. Kalantar, E. Bringa, M. Caturla, J. Colvin, K. T. Lorenz,

M. Kumar, J. Stolken,

**Lawrence Livermore National Laboratory**

A. M. Allen, K. Rosolankova, J. S. Wark

*University of Oxford*

M. A. Meyers, M. Schneider

*University of California, San Diego*

T. R. Boehly

*University of Rochester, Laboratory for Laser Energetics*

Laser-based shock experiments have been conducted in thin Si and Cu crystals at pressures above the Hugoniot Elastic Limit (HEL). In these experiments, static film and x-ray streak cameras recorded x-rays diffracted from lattice planes both parallel and perpendicular to the shock direction. This data showed uniaxial compression of Si (100) along the shock direction and 3-D compression of Cu (100). In the case of the Si diffraction, there was a multiple wave structure observed, which may be due to a 1-D phase transition or a time-variation in the shock pressure.

A new film-based detector has been developed for these in-situ dynamic diffraction experiments. This large-angle detector consists of 3 film cassettes that are positioned to record x-rays diffracted from a shocked crystal anywhere within a full π-steradian. It records x-rays that are diffracted from multiple

lattice planes both parallel and at oblique angles with respect to the shock direction. It is a time-integrating measurement, but time-resolved data may be recorded using a short duration laser pulse to create the diffraction source x-rays.

This new instrument has been fielded at the OMEGA and Janus lasers to study single crystal materials shock compressed by direct laser irradiation. In these experiments, a multiple wave structure was observed on many different lattice planes in Si. This data provides information on the structure under compression.

**Introduction**

When a material is shock compressed at a very low pressure, it typically responds by deforming elastically. At a pressure above the Hugoniot Elastic Limit, it deforms plastically. This plastic deformation of materials is often characterized by a semi-empirical model such as the Steinberg-Guinan model [1]. Constitutive models such as this have been developed by fitting to shock data that was recorded at low strain rates from $10^3$-$10^5$ $s^{-1}$, such as obtained with a gas gun. They do not describe the microscopic physics that occurs in order for that plastic deformation to take place.

When the solid undergoes deformation at high pressure, stresses that occur in the lattice initiate and propagate dislocations [2, 3]. The movement of the dislocations results in the rearrangement of the structure, which is plastic material flow. The number density of dislocations that are generated and the speed with which they propagate are dependent on the rate of the applied strain.

In order to study the detailed response of a material to shock loading, it is important to study the response of the lattice using *in-situ* dynamic x-ray diffraction [4-6].

High intensity lasers provide a capability to access high-pressure states of material, with diagnostic capabilities that are not available on other facilities. In particular, large lasers with multiple beams provide both a high-pressure capability and x-ray diagnostic capability. We have performed a series of experiments using the Nova and OMEGA lasers to study the deformation of single crystals by *in situ* dynamic x-ray diffraction [7-9].

Recently, the technique of in-situ diffraction has been extended to provide simultaneous measurements of multiple lattice planes using a new detector. This is a large solid angle film-based detector that records x-rays diffracted from many different lattice planes to provide the detailed information necessary to diagnose the state of the material under compression.

This large-angle coverage detector is described in the context of adding information on the shock compressed lattice, and methods for data analysis are discussed.

**In-situ dynamic diffraction**

X-ray Bragg diffraction is a technique used to study the structure of a solid. Here, x-rays scattered from the atoms in the lattice constructively interfere when the incident angle with respect to the lattice plane satisfies the Bragg condition:

$$n\lambda = 2d \times \sin(\theta)$$

The x-rays are diffracted at an angle $\theta$ equal to the incident angle (relative to the lattice planes).

When the lattice undergoes a deformation due to shock compression, the lattice compresses, so the lattice spacing decreases. The Bragg diffraction condition is then met at a different angle determined by the new lattice spacing (Figure 1). The technique of in-situ dynamic x-ray diffraction has been used to probe shocked single crystals with x-rays as they undergo deformation by shock compression. An x-ray source is positioned very close to the crystal so that the crystal subtends a range of angles including the new Bragg angle. The shift in diffraction angle is then recorded as a spatial shift in the diffraction signal.

**Previous results**

Experiments have been conducted on the Nova and OMEGA lasers to study the shock response of Si and Cu. In these experiments, the single crystal samples were approximately 2 mm in size, with a thickness of 40 $\mu$m for the Si and 2 $\mu$m for the Cu. The single crystal was shock loaded either by indirect (x-ray) drive, or direct (laser) drive, and the sample was probed using x-rays generated by high intensity beams incident on a thin metal foil. A nearly monochromatic source of x-rays was created. These x-rays were then diffracted from the lattice planes of the crystal and recorded on both static film and x-ray streak cameras.

X-rays diffracted from the (004) planes of Si and (002) planes of Cu parallel to the shock propagation direction in the crystal were recorded with one detector. X-rays diffracted from the orthogonal (040) planes on Si and (020) planes of Cu were recorded with a separate detector.

In the case of single crystal Si (100), the sample was shock loaded to pressures up to approximately 120 kbar. X-rays diffracted from the (004) planes showed a dynamic response as the Bragg angle shifted, as illustrated in Figure 3. The shift of 1.85 Å x-rays from a Bragg angle of 42.95° to 46.72° indicates a compression of the 2d lattice spacing of approximately 6.4% along the shock direction. Simultaneous measurements of the orthogonal (040) lattice planes showed no response to the shock loading. In this case, the Si appears to respond uniaxially.

In the case of the single crystal Cu. These foils were shock compressed to a peak pressure of approximately 200 kbar. X-rays diffracted from the (002) and (020) lattice planes showed a compression of apprimately 2.5-3%, as illustrated in Figure 2. In this case, the broadening of the signal is thought to be due to a high density of dislocations as well as structure in the shock due to the laser drive on the very thin samples. The observed compression in both the Bragg and Laue measurements is consistent with a fully 3-dimensional compression of the Cu. This volumetric compression is a result of the local rearrangement of the lattice under compression due to the generation and propagation of dislocations. [9]

In the case of the single crystal Si work, the response of the lattice appears to be elastic, but it may also be consistent with a shock-induced phase transformation. At low pressure, the compression of the (004) planes is only a few %. At moderate pressure (100 kbar), several different compressions are

observed with a multi-wave structure. At higher pressures (>100 kbar), a single lattice compression of approximately 6.4% is observed. The fact that the compression remains at approximately 6.4% along the shock direction could correspond to the density at which a shock-induced phase transformation occurs, where the lattice spacing of the final state is not recorded.

In order to further study the response of the Si and other materials, a wide solid-angle collection detector was developed. This detector is described in detail in the following sections.

**Wide-angle detector**

The new wide-angle detector was developed to collect x-rays diffracted from multiple lattice planes. It consists of 3 separate static x-ray film holders, one rectangular in shape, and 2 triangular in shape.. These film holders are 71 mm x 142 mm in size. Each film holder has a 0.75 mm thick Be blast shield, and holds several layers of thin metal foil filters and 2 pieces of DEF film. These film holders are bolted together to approximate a 90° segment of a sphere. The geometry of the full assembly is shown in Figure 3.

This detector was designed for experiments at the OMEGA, laser at the University of Rochester, and has also been used at the Janus laser at LLNL. We describe the details of how it is configured and fielded at OMEGA. The detector is positioned in the OMEGA target chamber by inserting it in a TIM (Ten-inch-manipulator), and held so that it surrounds target chamber center, subtending an

angle of ≥90° in one direction and 180° in the other. It is placed so that the 3 separate film planes are located 53 mm from target chamber center.

This instrument is used in combination with a target designed specifically for wide-angle diffraction. The target is illustrated in Figure 4. It consists of a lead-doped plastic base plate that holds the single crystal sample, and a thin gold shield that holds a metal foil for the x-ray backlighter source. K-shell x-rays are created by 4-6 laser beams incident on the thin metal foil. The size of the source of x-rays is defined by a 200 $\mu$m diameter aperture in the backlighter shield.

The K-shell x-rays that diffract from the crystal are recorded on film. The direct line of sight to the film is blocked with a cylindrical shield placed above the 200 $\mu$m aperture. This provides x-rays over an angular range up to 180 x 90 degrees that may be incident on the crystal and diffracted to the film.

**Demonstration and analysis**

This new detector has been fielded on a series of target experiments at OMEGA. A preliminary test was done with single crystal Cu. X-rays diffracted from approximately 12 different lattice planes of the static Cu sample were recorded on film simultaneously, as shown in Figure 5. In this geometry, the crystal had a (001) orientation. It had an arbitrary orientation about the sample normal. A thin Cu foil was used for the x-ray source, providing x-rays with a wavelength of 1.49 Å. X-rays diffracted from the (002) planes have a Bragg angle of 24.36°, and from the (004) planes have a Bragg angle of 55.64°. Both of these

are visible, along with x-rays diffracted from planes at an angle with respect to the crystal surface.

The different lines that are visible in this sample image are conic sections. Each results from a point source of x-rays diffracted from a single lattice plane and recorded on a flat piece of film. The geometry to illustrate this is shown in Figure 6. In this illustration, x-rays diffracted from an arbitrary infinite lattice plane form the surface of a cone. The orientation of the lattice normal is the direction of the axis of the cone, and the Bragg angle for that lattice plane is 90 minus the half angle of the cone. The extent of the cone of x-rays diffracted from the crystal is determined by the angle that the crystal subtends to the x-ray source, and the appearance of the line on film is the intersection of this cone with the static film detector.

The process for identifying the lattice planes and extracting quantitative information on the shock response of the crystal is an iterative process that requires us to first identify the lattice planes, to transform the data to spherical coordinates, and then to fit the lattice planes for arbitrary diffraction signals.

The first step is to identify some of the lattice planes in the film data. This is done using an IDL code to calculate the expected signal from a given lattice plane. An x-ray source and lattice plane are input, and a diffraction pattern is calculated as an image that displays in spherical coordinates, theta and phi. An image that includes the diffraction signals from several different lattice planes may be calculated based on the selection rules for the particular crystal.

We show several calculated images in Figure 7 for single crystal Cu. In this case, we show only the diffraction for the (002), (004), (±1,-1,3), (±113), and (±313) planes. Two cases are shown, for the rotation of the crystal oriented

symmetrically with respect to the film, and for a slight offset rotation of 20°. By comparing the film images with the calculated diffraction patterns, a number of lattice planes are identified. These are then used to optimize the relative position of the target with respect to the film for the detailed lattice plane analysis.

In this case, the (002) and (004) planes are used. For an x-ray source with a wavelength of 1.49 Å, the Bragg angle for the (002) plane is 24.36°, and for the (004) plane is 55.64°. An IDL code is used to warp the film images to spherical coordinates based on geometrical inputs such as the position and angle of the crystal relative to the film. This transformation is optimized to match the Bragg angles for both the (002) and (004) planes. The optimum transformation is shown in Figure 8. Note that in spherical coordinates, the (002) and (004) planes are located at fixed values of theta.

The final step is to extract lattice information from other planes. This is done by identifying several points on each line, and fitting a conic section to those points. The parameters for this conic section then define the lattice plane. Specifically, the half-angle of the best-fit cone is 90-Bragg angle, and the axis of the cone is directed along the unit normal for the specific lattice plane (Figure 6). Note that in this example of a static Cu crystal, the other planes should match the planes for single crystal Cu.

We have performed this fitting for a few planes for illustration. The results are summarized in Figure 9. In this case, the fit parameters for the (313) plane are evaluated. The best-fit cone indicates a lattice spacing of 1.66 Å, which compares closely with the actual spacing of 1.72Å.

**Shock experiments**

This process of analysis may be applied to shock data provided both the preshock and shock diffraction signals are recorded on the film. The preshock image provides the data to optimize the transformation to spherical coordinates, and then the shock data provides information on the actual lattice configuration under shock loading. This is illustrated in Figure 10. Here, x-rays diffracted from multiple lattice planes of Si were recorded during a shock experiment. A multiple-line structure is observed for many different lattice planes. This corresponds to both the unshocked and shocked Si lattice.

Preliminary analysis of the diffraction lines in this image shows a compression of the (004) lattice planes by 6.4%. Other lattice planes also show compression. The details of the compression for each lattice plane will be used to identify the lattice response due to this dynamic loading process.

**Advanced concepts**

There are several different ways that this large-angle detector may be used. In the experiments that we describe above, the duration of the x-ray source for diffraction is 4 ns, determined by the length of the laser pulse. Shorter time-resolution may be achieved with a shorter duration laser pulse. On OMEGA, this may be a 200 ps impulse. It is also possible to use a short (ps) pulse for fast time-resolution. In general, this requires multiple shots to acquire a detailed understanding of the dynamic response of the lattice.

In these experiments, it is critical to calibrate the lattice orientation with respect to the film. We have done this in the example data using the unshocked lattice diffraction pattern. In the case where a shorter laser pulse is used to probe the lattice, multiple beams may be used to create a double pulse backlighter to record a preshock image of the diffraction pattern, as well as a diffraction pattern during shock loading. This may be extended to include multiple images at different times during the shock loading provided the different patterns may be resolved and distinguished. One concept for this is to use separate foils for the x-ray backlighters. By designing the target with two separate backlighter foils and apertures, images may be recorded at different times with different wavelength x-ray diffraction sources. For example, Fe and Cu may be used to probe a sample of Cu (111). In this case, the Bragg angle for the Fe x-rays is 62.8°, and for the Cu x-rays is 45.8°. The diffracted lines can be distinguished with differential filtering in the film pack to allow detailed fitting of the preshock vs. shock response of the lattice. This concept is illustrated in Figure 11.

The large-angle collection detector allows us to record x-rays diffracted from many different lattice planes. This may be used for poly-crystalline samples with large grains. Since the x-rays are incident at a wide range of angles on the crystal, this is not useful as a diagnostic of the detailed lattice structure for a poly-crystal material, but it does provide a diagnostic of the state of the material by the existence of a lattice. This is demonstrated with images of poly-crystalline Be, shown in Figure 12. A pattern of diffraction lines is evident, indicating that this material is solid during the experiment.

**References**


[1] D. J. Steinberg, S. G. Cochran, and M. W. Guinan, J. Appl. Phys. **51**, 1498-1504 (1980).

[2] E. Zaretsky, J. Appl. Phys. **78**, 1 (1995).

[3] L. C. Chhabildas and J. R. Asay, J. Appl. Phys. **50**, 2749 (1979).

[4] Q. Johnson, A. Mitchell, and L. Evans, Nature (London) 231, 310 (1971); Q. Johnson, A. Mitchell, and L. Evans, Appl. Phys. Lett. 21, 29 (1972).

[5] J. S. Wark, R. R. Whitlock, A. A. Hauer, *et al*, Phys Rev B 40, 5705 (1989).

[6] E. Zaretsky, J. Appl. Phys. **78**, 1 (1995); P. A. Rigg and Y. M. Gupta, Appl. Phys. Lett. **73**, 1655 (1998

[7] D. H. Kalantar, E. A. Chandler, J. D. Colvin, *et al*, Rev. Sci. Instrum. **70**, 629 (1999).

[8] D. H. Kalantar, B. A. Remington, J. D. Colvin, *et al*, Phys. Plasmas **7**, 1999 (2000).

[9] A. Loveridge-Smith, A. Allen, J. Belak, *et al*, Phys. Rev. Letters **86**, 2349 (2001).



This work was performed under the auspices of the U.S. Department of Energy by the University of California, Lawrence Livermore National Laboratory under Contract No. W-7405-Eng-48.

# Figure 1

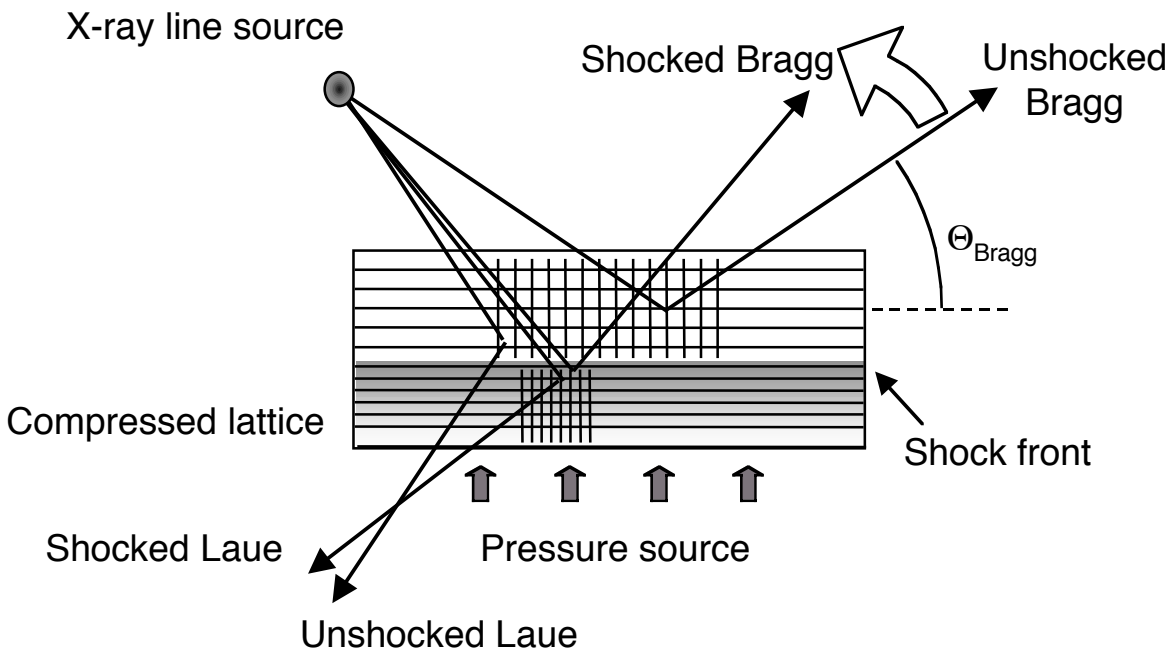
X-ray line source
Shocked Bragg
Unshocked Bragg
$\Theta_{Bragg}$
Compressed lattice
Shock front
Shocked Laue
Pressure source
Unshocked Laue

# Figure 2

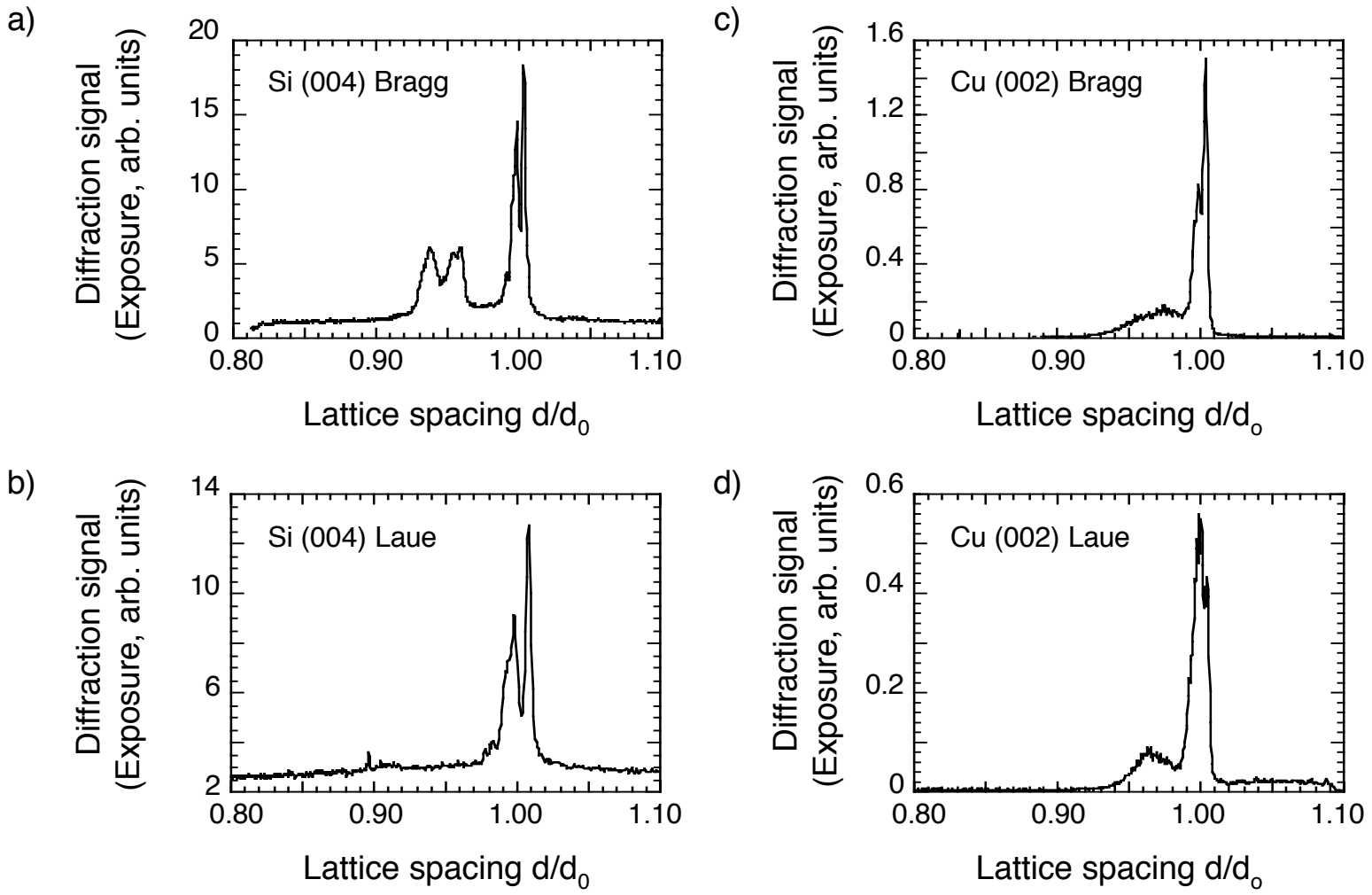
a)
Diffraction signal
(Exposure, arb. units)
Si (004) Bragg
20
15
10
5
0
0.80
0.90
1.00
1.10
Lattice spacing d/d0
c)
Diffraction signal
(Exposure, arb. units)
Cu (002) Bragg
1.6
1.2
0.8
0.4
0
0.80
0.90
1.00
1.10
Lattice spacing d/do
b)
Diffraction signal
(Exposure, arb. units)
Si (004) Laue
14
10
6
2
0.80
0.90
1.00
1.10
Lattice spacing d/d0
d)
Diffraction signal
(Exposure, arb. units)
Cu (002) Laue
0.6
0.4
0.2
0
0.80
0.90
1.00
1.10
Lattice spacing d/do

# Figure 3

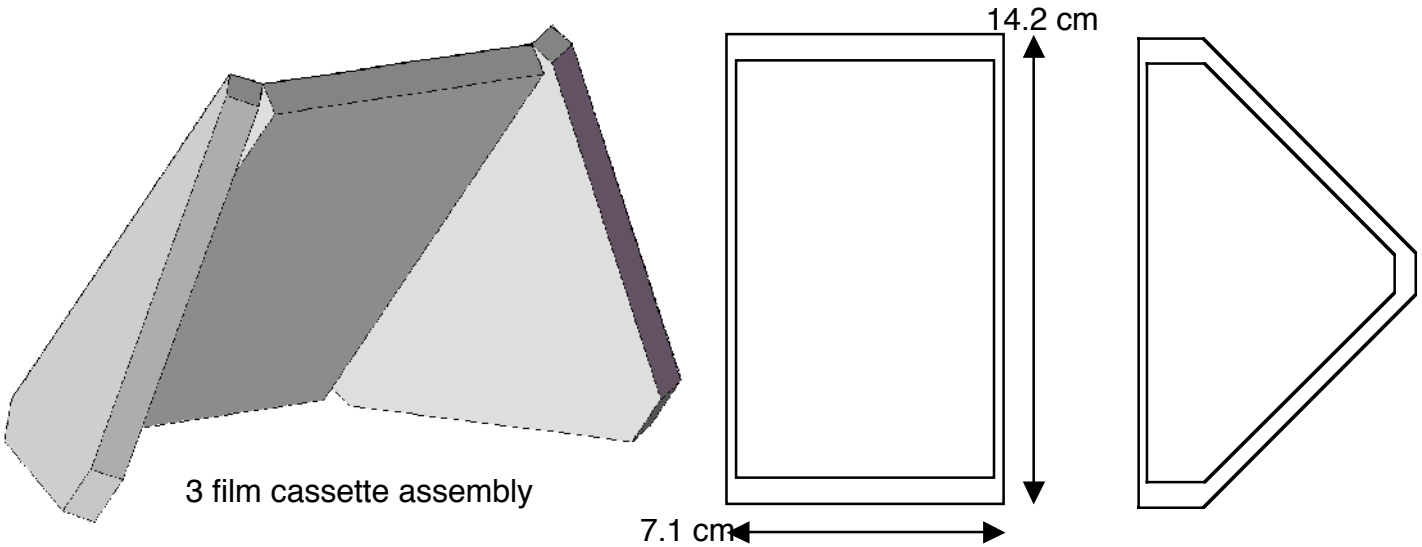

# Figure 4

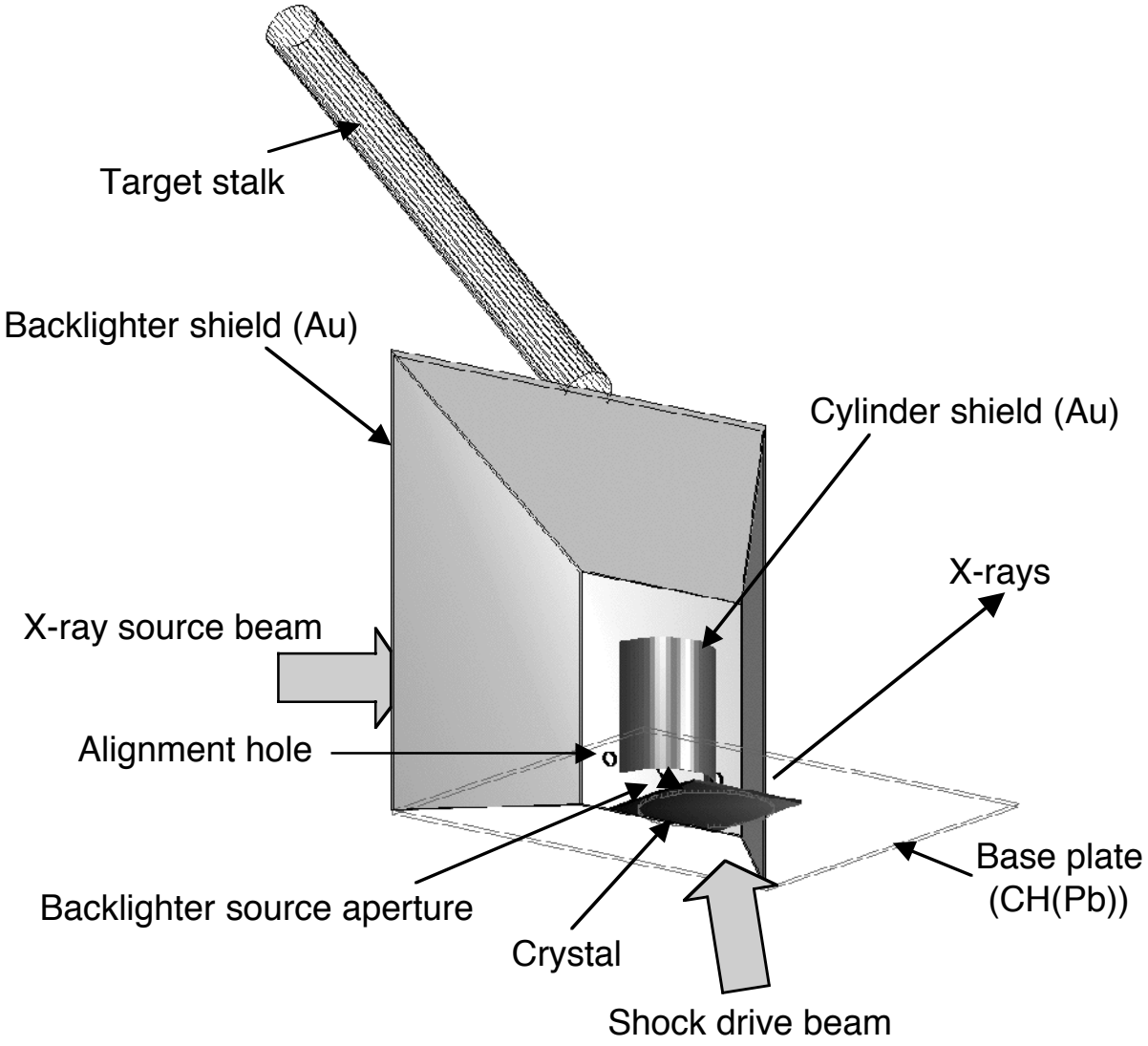
Target stalk
Backlighter shield (Au)
Cylinder shield (Au)
X-rays
X-ray source beam
Alignment hole
Backlighter source aperture
Crystal
Base plate
(CH(Pb))
Shock drive beam

# Figure 5

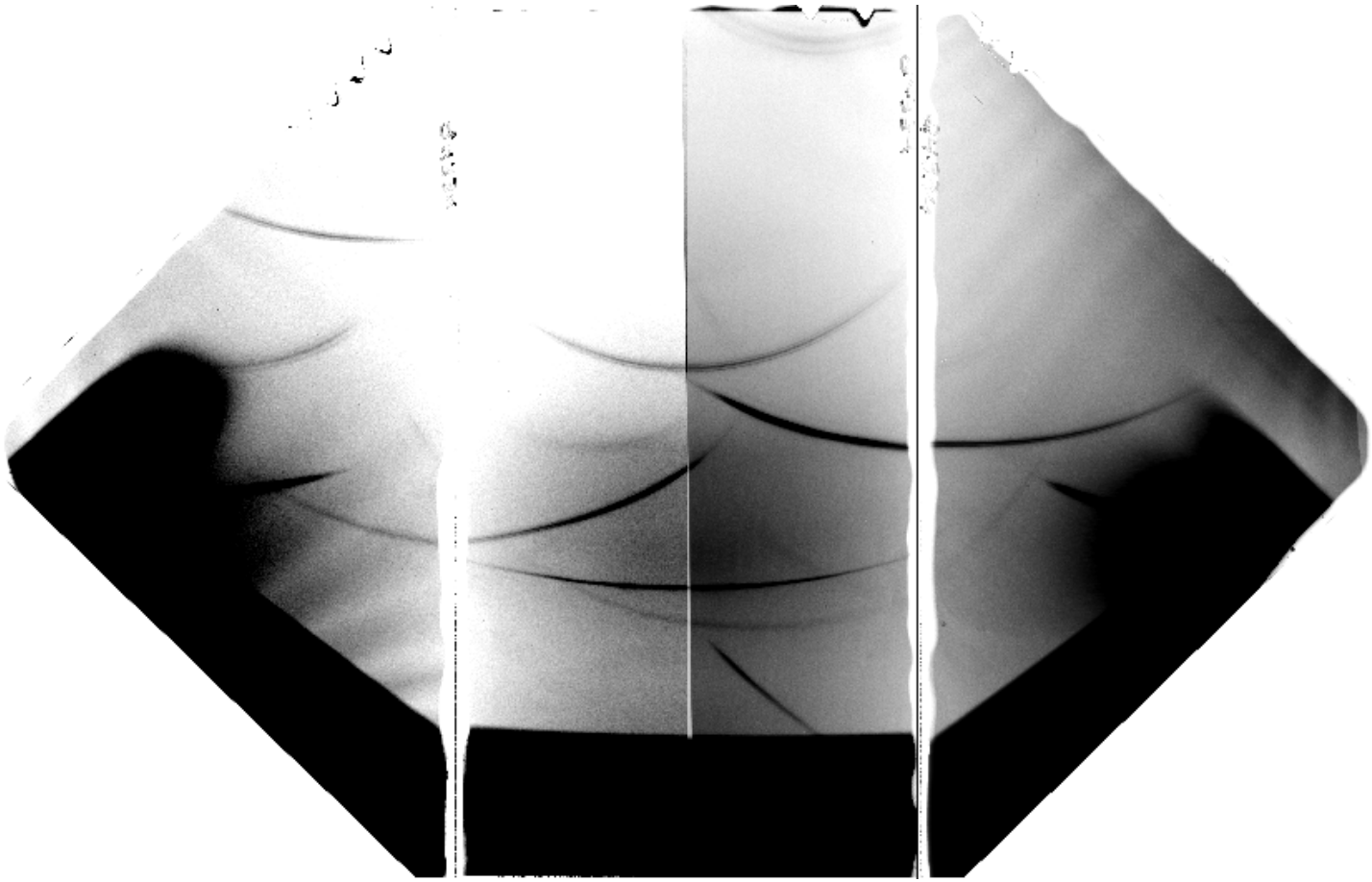

# Figure 6

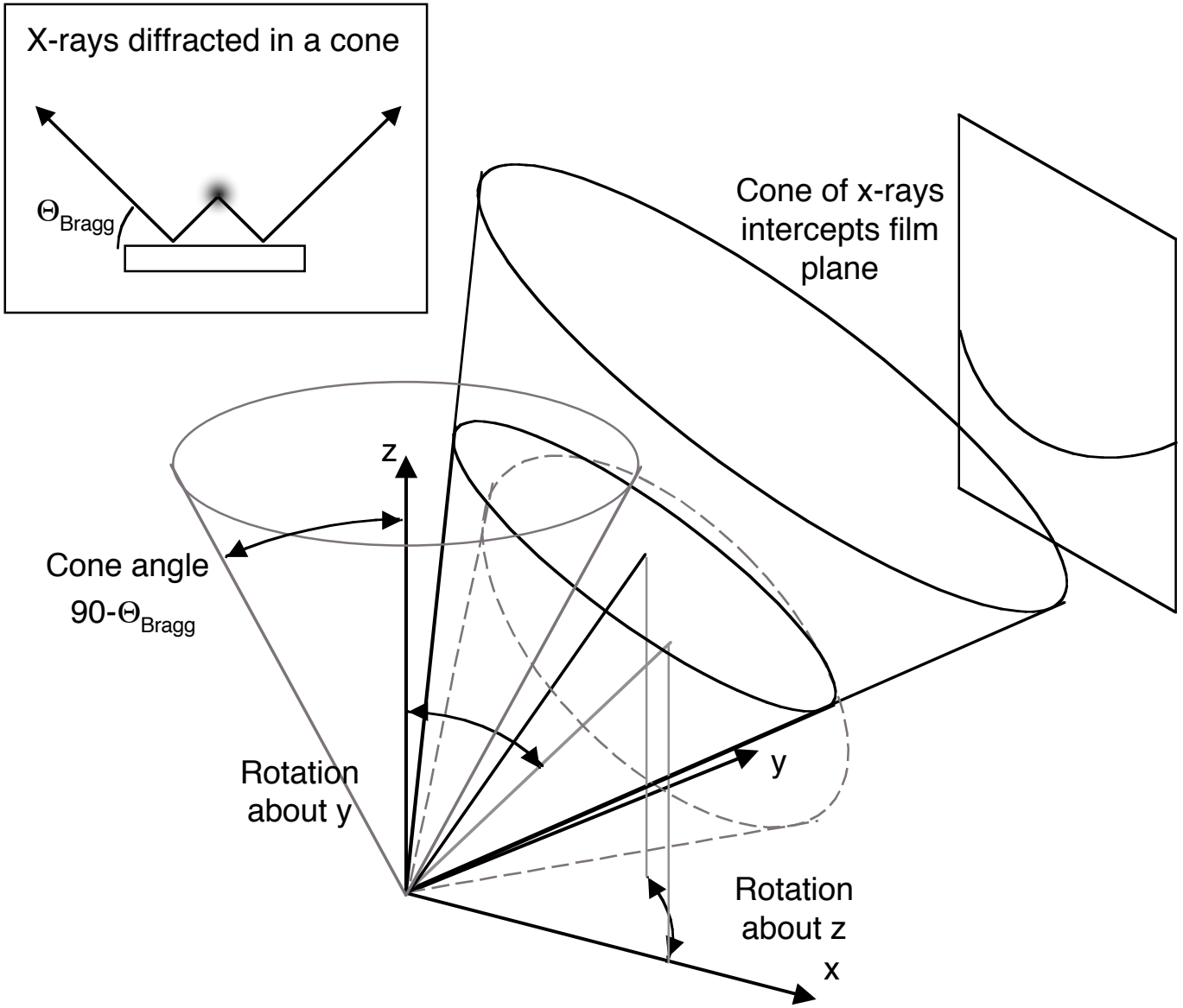
X-rays diffracted in a cone
$\Theta_{Bragg}$
Cone of x-rays intercepts film plane
z
Cone angle
90-$\Theta_{Bragg}$
Rotation about y
y
Rotation about z
x

# Figure 7

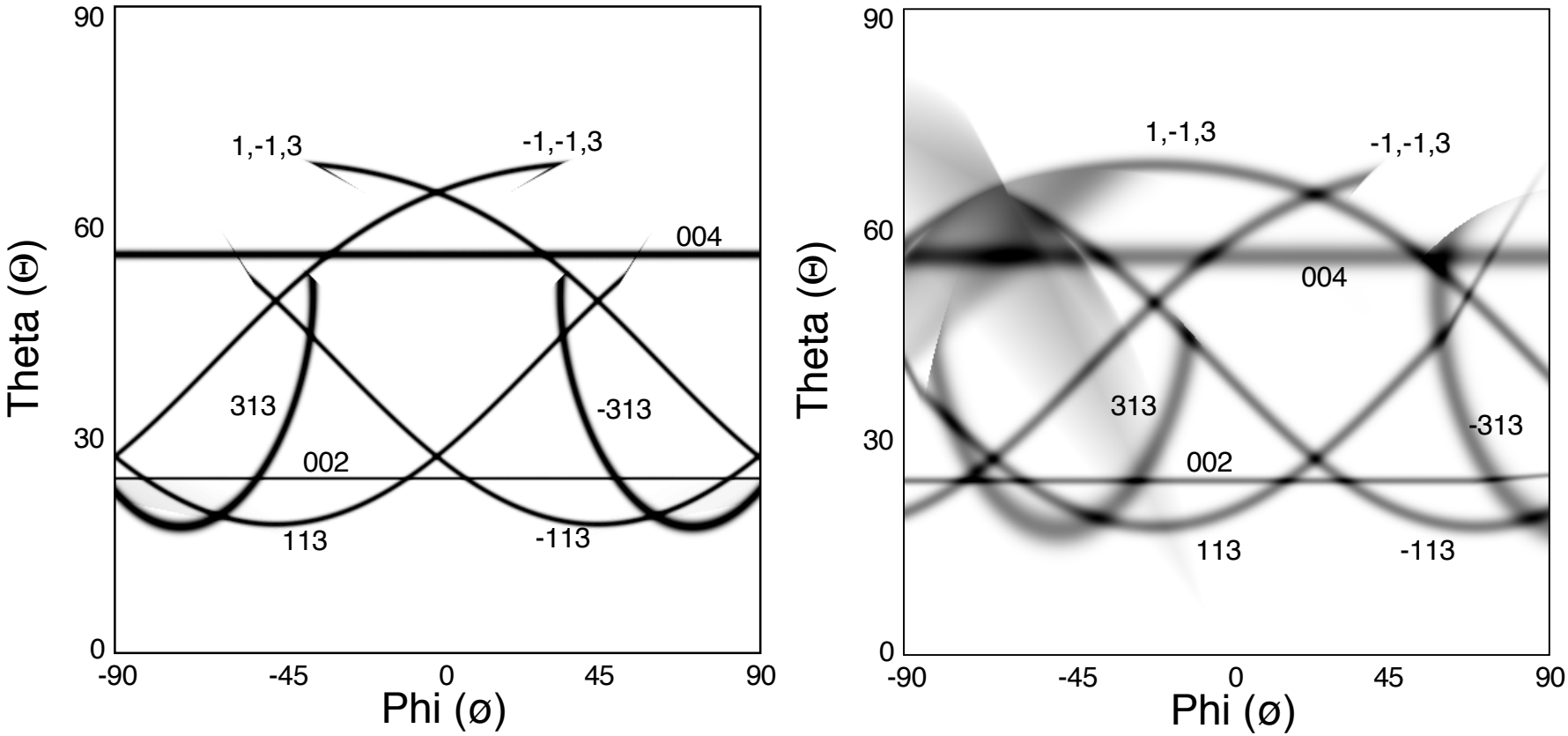
90
60
30
0
Theta (Θ)
1,-1,3
-1,-1,3
004
313
-313
002
113
-113
-90
-45
0
45
90
Phi (ø)
90
60
30
0
Theta (Θ)
1,-1,3
-1,-1,3
004
313
-313
002
113
-113
-90
-45
0
45
90
Phi (ø)

# Figure 8

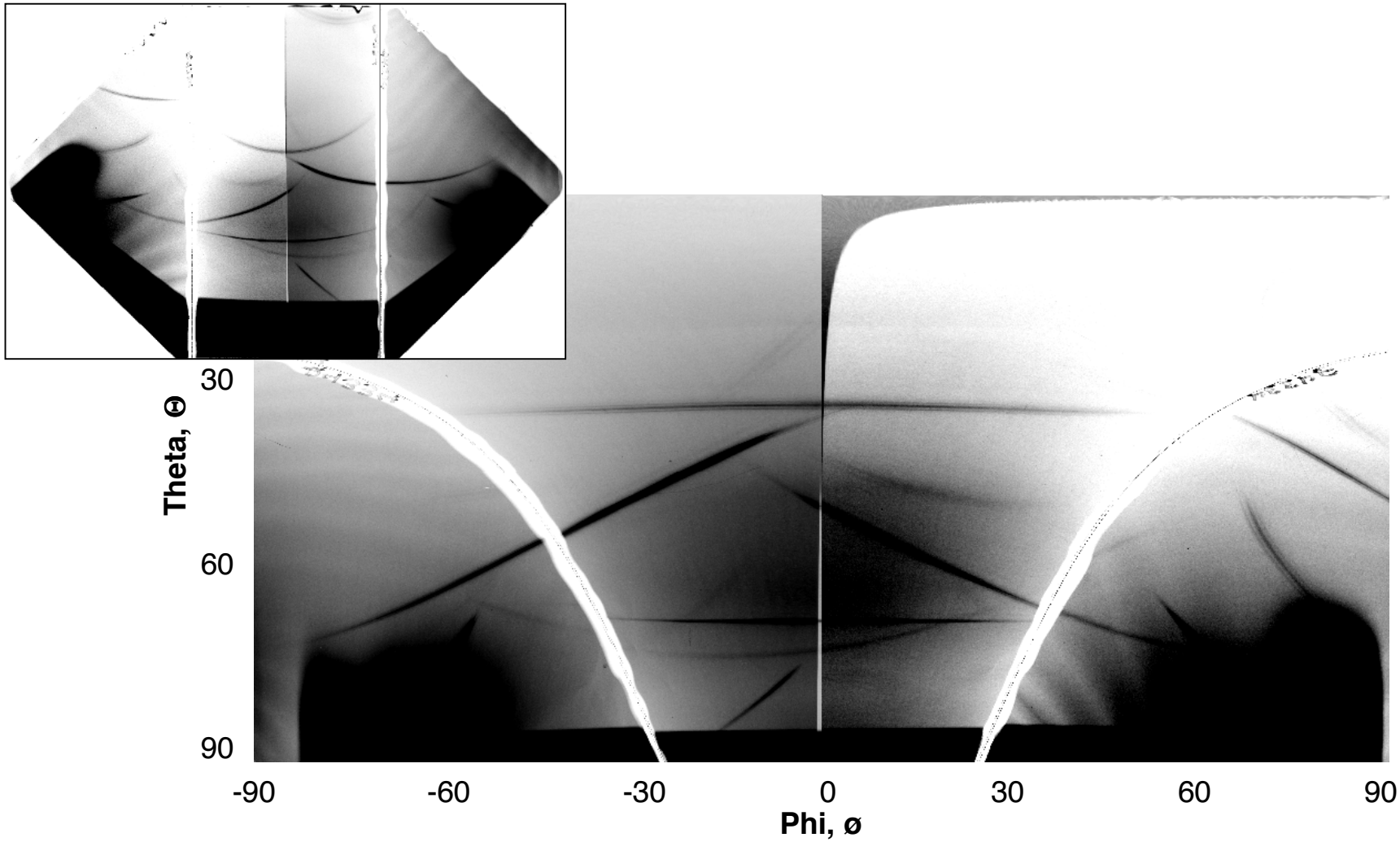

# Figure 9

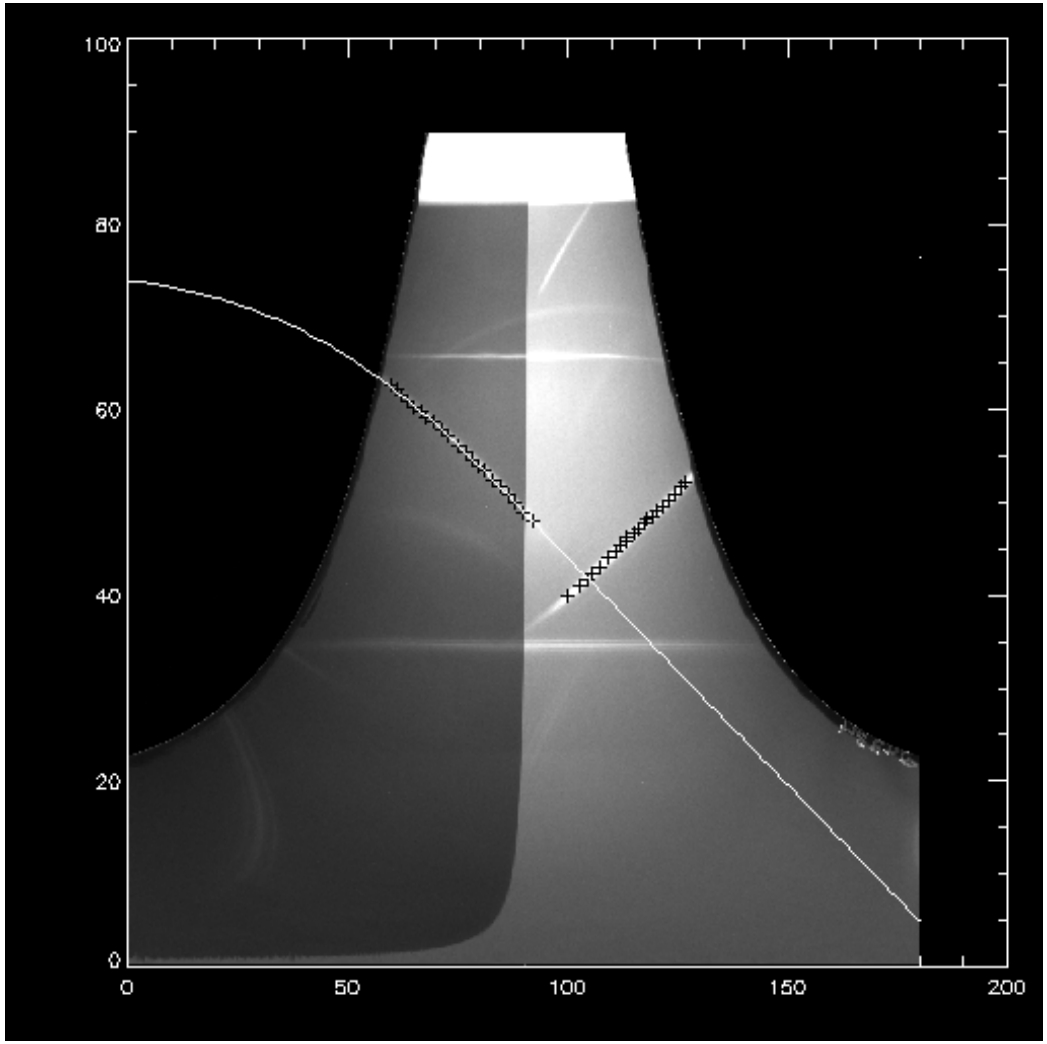

# Figure 10

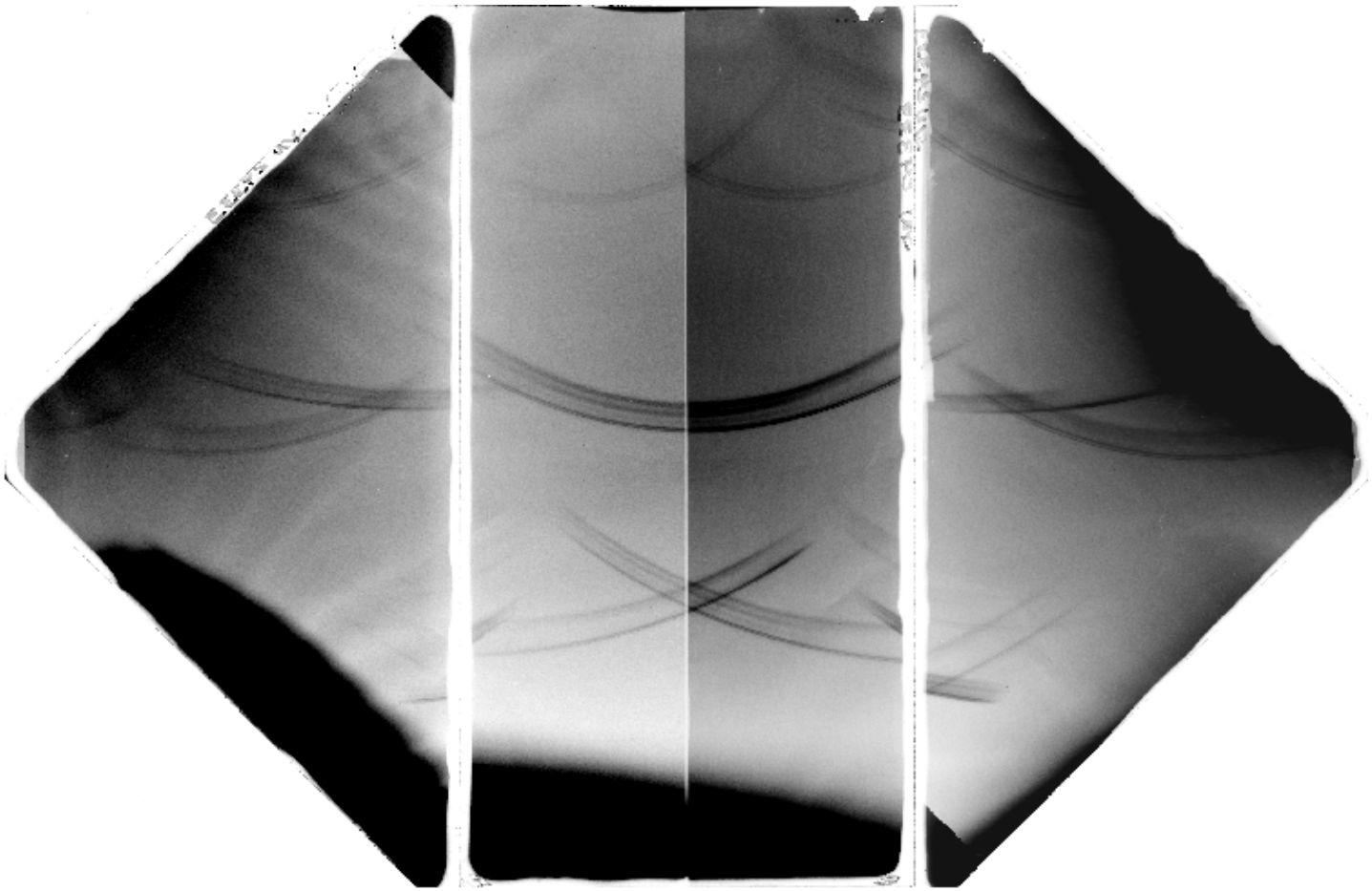

# Figure 12

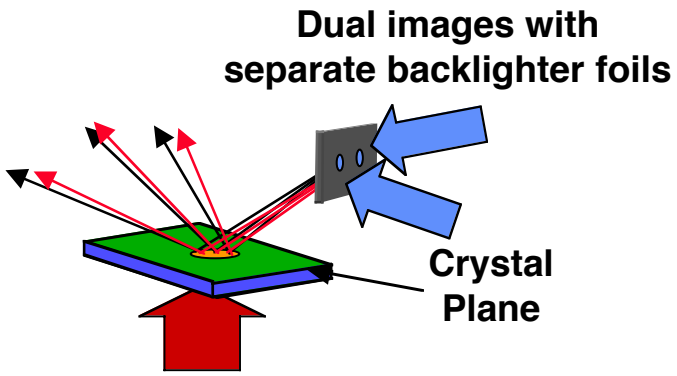
Dual images with
separate backlighter foils
Crystal
Plane

# Figure 13